Uniport Journal of Engineering and Scientific Research (UJESR)

Vol. 5, Issue 2, 2021, Page 13-22
ISSN: 2616-1192

(www.ujesr.org)

Wide Angle Radar Absorption Characteristics of Cross-Block Structured Absorber with Metamaterial Features

Abdullahi, M.B[*1,2], Ali, M.H[*1] and Gana, U.M[1]
[1]Department of Physics, Bayero University Kano Nigeria
[2]Department of Physics, Usmanu Danfodiyo University Sokoto Nigeria
*Corresponding authors' emails: abdullahi.bello@udusok.edu.ng; mhali.phy@buk.edu.ng

Abstract
In this study, a broadband and wide-angle cross-block structured radar absorbing material (RAM) with metamaterial features based on flaked carbonyl iron magnetic composite is presented. The unit cell of the structure was designed and simulated on Comsol Multiphysics to determine its frequency dependent absorption characteristics under oblique incidence. Chew's reflection coefficient for oblique incidence expression was used to theoretically evaluate the absorption response of the designed structure. The simulated and calculated reflectivity results showed stability under oblique incidence. The simulated results also revealed broadband absorption with effective bandwidth of 9.4 GHz for transverse electric (TE) and transverse magnetic (TM) polarizations for angles of incidence ranging up to 45^0 displaying absorptivity greater than 80%. The relative bandwidth of this RAM was found to be 5.29 at normal incidence and 4.35 at 45^0 incidence, making it better than the recently reported one with a value of 2.24 at normal incidence and 1.12 at 45^0 incidence for TE polarization, thus contributing significantly in overcoming the challenging demand of broadband, wide angle and thin thickness requirements for practical applications.

Keywords: *Metamaterial, Radar, Reflectivity, Relative Bandwidth, Wide-Angle*

Received: 30th June, 2020 *Accepted: 3rd January, 2021*

1. Introduction

Radar absorbing materials (RAMs) have been extensively studied in the last few decades due to their uses in the field of defense such as reduction of radar visibility in different types of targets and civilian applications like shielding circuits from unwanted interference in a broad range of electromagnetic frequencies(Abdalla, 2013; Kapelewski, 2013; Wan et al., 2015). These applications require wide operating frequency, thus multiband and broadband absorbers are increasingly required in this age. Conventional RAMs are found wanting in practical applications owing to their increased thickness and weight (Ranjan et al., 2018) resulting from multiple layers incorporation while attempting to broaden the working frequency range of such RAMs. Besides, the search and development for new stealth materials seems to have reached a deadlock due to limitations in their intrinsic complex electromagnetic parameters (Zhou et al., 2016). Ideally, RAMs characteristics includes broadband, ultra-thin thickness, lightweight and efficient absorption properties (Haitao et al., 2018) that are challenging to realize simultaneously.

Recently, artificially engineered subwavelength periodic structures that exhibit exotic and fascinating behaviours unavailable in naturally occurring materials are considered as potential route to finding ultrathin and light weight RAMs (Zhou et al., 2016). In lieu of these interesting properties, many metamaterial devices have been researched in relevant spectral range from radio (Wiltshire et al., 2001), microwave (Edwards et al., 2009; Smith et al., 2000), to THz (Hokmabadi et al., 2013; Tao et al., 2008a; Tao et al., 2008b), infrared (Liu et al., 2011) and visible (Mulla and Sabah, 2015). The first near unity absorption metamaterial absorber (MMA) was reported in 2008 (Landy et al., 2008). These MMAs are designed by the use of inclusions that interact in a resonant manner with the electromagnetic wave propagating in the metamaterial. Thus, the bandwidth of these MMAs were generally very narrow, usually around the resonance frequency (Pang et al., 2012), which hinder their application

in practice. To broaden the absorption band, various designs and methods have been reported such as but not limited to, replacing the dielectric substrate in the traditional metal-dielectric-metal MMAs with a magnetic media (Nguyen and Lim, 2018), which proved to be as an effective approach to achieve multiple resonances and broadband absorption in a relatively thinner material (Xiao et al., 2019; Xu et al., 2015; Zhang et al., 2015).

In the last decade, some works have been put forward on the magnetic medium based metamaterial absorbers (Cheng et al., 2014 & 2016; Li et al., 2018). These studies reported that magnetic substrate based MMAs recorded incredible progress in overcoming the challenging task of attaining idealized characteristics of RAMs under normal incidence of the wave. Only very few reports (Chen et al., 2016; Cheng et al., 2016; Haitao et al., 2018; Li et al., 2018) paid attention to oblique incidence which is an essential requirement for practical application of absorbers. It is worth mentioning that, an aircraft receives incident waves from the radar network systems at oblique angles up to 60^0 (Wong et al., 2006). Moreover, the relative bandwidth at incident angle of 45^0, is very small or absent in the very few reports that investigated oblique incidence property of their model absorbers. Furthermore, minimization of the overall reflectivity in a specific frequency band and a specific range of angles of incidence for any polarization remains an unsolved problem.

Consequently, a broadband radar absorbing material configuration with metamaterial features based on magnetic substrate earlier presented in our report (Abdullahi and Ali, 2019) was studied under oblique incidence in this paper. Chew's reflection coefficient (Dib et al., 2010) was utilized to evaluate the absorber performance at oblique incidence. The influence of angle of incidence on the absorption performance of RAM was analyzed. The power loss density from the simulation is used to explain the physical absorption mechanism of the absorber. Finally, both simulated and calculated results showed that the proposed RAM maintains broad bandwidth exhibiting below -10dB reflectivity thereby demonstrating relatively stable bandwidth within a wide range of angles of incidence.

2. Theoretical considerations

For a multilayer absorber with an oblique incident transverse electric (TE) polarized wave like the one being reported, the generalized reflection coefficient at an interface between layer i and layer $i+1$ is expressed as follows (Dib et al., 2010):

$$\tilde{R}_{i,i+1} = \frac{R_{i,i+1} + \tilde{R}_{i+1,i+2} e^{-j2k_{i+1,z}\, d_{i+1}}}{1 + R_{i,i+1} \tilde{R}_{i+1,i+2} e^{-j2k_{i+1,z}\, d_{i+1}}} \quad (1)$$

Evaluating Equation (1) recursively starting from $\tilde{R}_{N-1,N}$ to $\tilde{R}_{01}$, the total reflection coefficient of the multilayer absorber can be obtained at any angle of incidence. From equation (1), it is required to find $R_{i,i+1}$ for any layer under consideration which is presented as Equations (2) and (3) for TE and TM (transverse magnetic) polarizations respectively (Dib et al., 2010).

$$R_{i,i+1} = \frac{\mu_{i+1}k_{i,z} - \mu_i k_{i+1,z}}{\mu_{i+1}k_{i,z} + \mu_i k_{i+1,z}} \quad (2)$$

$$R_{i,i+1} = \frac{\varepsilon_{i+1}k_{i,z} - \varepsilon_i k_{i+1,z}}{\varepsilon_{i+1}k_{i,z} + \varepsilon_i k_{i+1,z}} \quad (3)$$

where ε_i and μ_i are the complex permittivity and permeability, accordingly for the i^{th} layer. $k_{i,z} = k_i \cos(\theta_i)$ where θ_i is the angle of transmission in the i^{th} layer. In terms of angle of incidence θ at the absorber-air interface, $k_{i,z}$ is given by Equation (4) (Dib et al., 2010).

$$k_{i,z} = \omega\sqrt{\mu_i\varepsilon_i - \mu_0\varepsilon_0 sin^2\theta} \quad (4)$$

where μ_0 and ε_0 retains their usual meanings.

Effective electromagnetic parameters of the structured layers can be obtained using Equation (5), which is based on strong fluctuation theory of honeycomb-structured surfaces (Zhou et al., 2016).

$$\varepsilon_{eff} = \frac{1}{2}[(1-2g)(1-\varepsilon_r) + \sqrt{(1-2g)^2(1-\varepsilon_r)^2 + 4\varepsilon_r} \quad (5)$$

where ε_{eff} is the effective permittivity, g is the volume ratio of the solid part in a layer, and ε_r is the permittivity of the solid. Effective permeability μ_{eff} can be obtained by replacing ε_r with μ_r in equation (5). An equation obtained from reflection theory model (Yang et al., 2017) and presented as Equation (6) was employed to explain the physical absorption mechanism of the modelled structure.

$$A(\omega) \propto -\omega\, \mu'\, d\, cos\theta \quad (6)$$

where ω is the angular frequency, μ' is real permeability, d is the thickness of the dielectric while θ is the angle of incidence.

3. Materials and methods

This consists of numerical validation of the Comsol Multiphysics simulation software, structure design, absorber simulations as well theoretical verification of the proposed absorber. The simulation was carried out in COMSOL Multiphysics environment.

3.1 Comsol multiphysics software validation

Finite element method (FEM) based COMSOL Multiphysics simulation package was used for numerical modeling of the proposed radar absorbing material with metamaterial features. In order to validate the COMSOL Multiphysics software, a metamaterial absorber which was numerically and experimentally realized by Li et al. (2018) using finite difference time domain (FDTD) solver CST Microwave Studio, was replicated on the COMSOL Multiphysics solver.

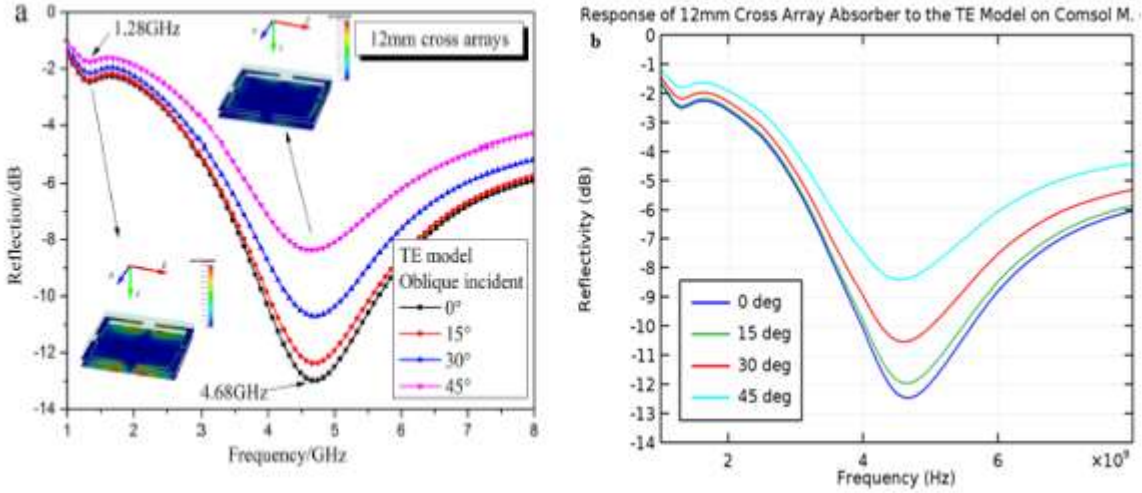

Fig. 1: Reflectivity of 12mm cross array absorber for TE (a) Li *et al.* (2018) (b) COMSOL Multiphysics

Simulation results of the 12mm cross array low frequency and broadband metamaterial absorber proposed by Li *et al* (2018) is represented in Fig. 1 alongside simulated results of COMSOL Multiphysics. The simulation results for both methods are identical for all the incident angles considered as shown in Figure 1. This confirms the reliability and accuracy of the COMSOL Multiphysics numerical solver used for the present work.

3.2 Design and simulation of the structure

The optimized geometric structure of a single unit cell of the proposed radar absorbing material is shown in Fig. 2. It consists of three layers of flaked carbonyl iron powder materials with a copper plate ground plane. The surface layer is cross shaped, the middle layer is a block shape structure and the bottom layer is considered as a conventional single slab absorber. The geometric dimensions of the RAM unit cell are optimized by using COMSOL Multiphysics' in-built Nelder-Mead method to ensure minimized reflectivity in the operational frequency band. The thickness of the bottom copper metallic plate was designed to be greater than the skin depth of the copper under the studied frequency intervals (2-18 GHz) so that it does not transmit any radiation.

The frequency dependent absorption response of the designed absorber is analyzed by the frequency domain solver of the simulation software. The absorber design in this work is for radar applications, therefore the frequency range of 2-18 GHz was considered. The electromagnetic parameters of the flaked carbonyl iron powder as measured by (Xu et al., 2015) are imported in to the simulation software to define the frequency dependent material properties using interpolation tool. The boundary conditions along x and y axes are chosen to be perfect magnetic conductor (PMC) and perfect electric conductor (PEC) which set tangential fields to 0 (Luo et al., 2019) are respectively applied to mimic an infinite periodic structure of the proposed RAM; whereas periodic port is used to input oblique incident plane polarized electromagnetic wave along z axis plane. Impedance boundary condition (IBC) which treats any material behind the boundary as being infinitely large is chosen for the ground plane. Physics controlled tetrahedral meshing is used in

the simulation while the output of the simulation software is the scattering parameters (s −parameters).

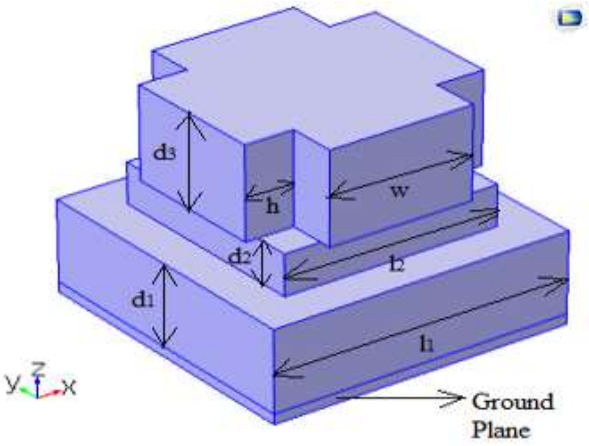

Fig. 2: Designed unit cell structure of the proposed RAM having metamaterial features geometric dimensions: $l_1 = 5.0mm$, $l_2 = 3.6mm$, $w = 2.4mm$, $h = 0.8mm$, $d_1 = 1.6mm$, $d_2 = 0.8mm$, $d_3 = 1.8mm$ and $ground\ plane\ thickness = 0.036mm$.

3.3 Theoretical evaluation of the structure reflectivity characteristics

Effective electromagnetic parameters of the surface and middle layers were calculated using strong fluctuation theory of honeycomb-structured surfaces given in Equation (5). The volume ratio (g) of the middle layer was obtained as 0.5184 by using $g = \frac{l_2^2}{l_1^2}$. The cross-shaped surface layer volume ratio was calculated as 0.5376 using $g = \frac{w^2+4hw}{l_1^2}$. These values are then used in Equation (5) to evaluate effective electromagnetic parameters of the surface and middle layers. Subsequently, $\tilde{R}_{i,i+1}$ in Equation (1) was evaluated recursively in order to finally calculate the model absorber reflectivity. The calculated reflectivity is then compared with the simulated reflectivity in order to validate the performance of the designed RAMM. The electromagnetic parameters of the flaked carbonyl iron powder as measured by (Xu et al., 2015) are used for the bottom layer.

4. Results and discussion

Reflectivity spectra of the model absorber was first studied under normal incidence for transverse electric (TE) and transverse magnetic (TM) polarizations. As depicted in Figure 3, the simulated reflectivity is the same for both TE and TM polarizations just as demonstrated by the calculated reflectivity results. The observed phenomenon agrees with the general conjecture that both polarizations should have the same magnitude of reflectivity for the case of normal incidence (Dib et al., 2010). Moreover, there is good agreement between the simulated and calculated results as indicated in Fig. 3 which confirms the reliability of the simulated results and the validity of the present design. The bandwidth of below -10dB reflectivity is 14.6 GHz (3.4-18 GHz) for the simulated and 15.0 GHz (3.0-18 GHz) for the calculated. In practice, electromagnetic wave usually strikes the absorber at an oblique incidence. As a result of this, the reflection spectra under different incident angles were presented in Figures 4a, 4b and 6a for the TE wave and Fig. 5a, 5b and 6b for the TM wave. For both waves, the incident angle was changed from 0^0 to 45^0 with a step of 5^0.

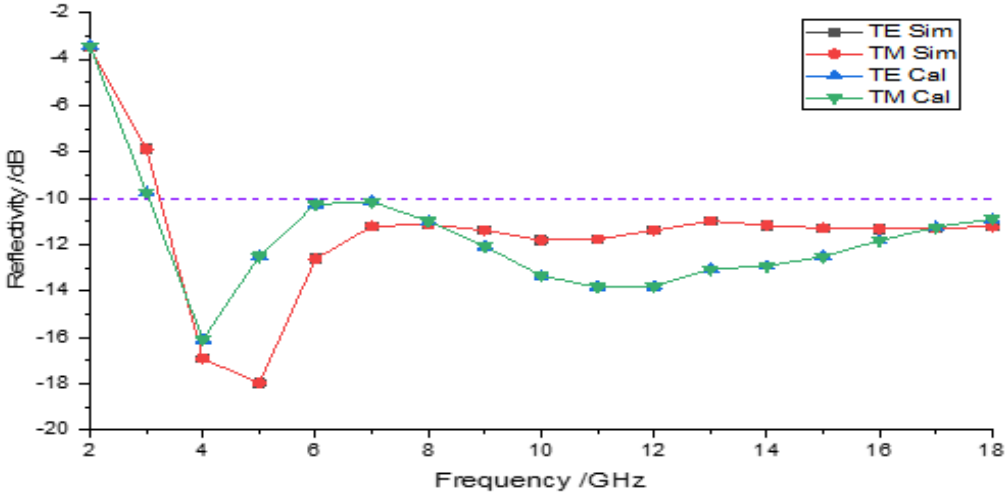

Fig. 3: Simulated and calculated reflectivity plots for TE and TM polarizations at normal incidence

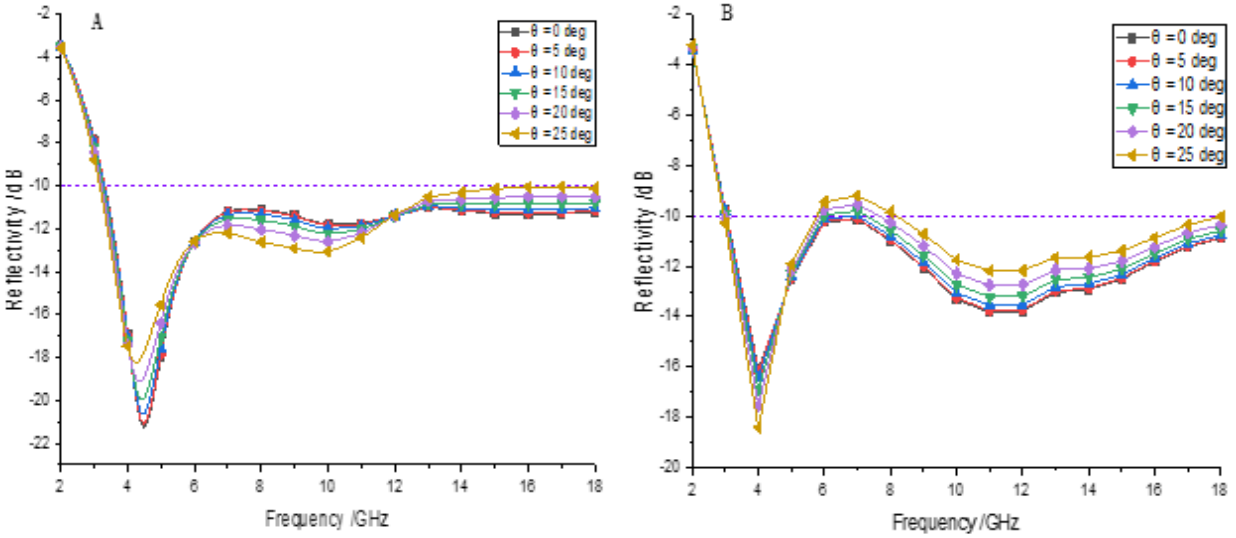

Fig. 4: Reflectivity plots for TE polarization at oblique incidence (a) simulated (b) calculated

Simulation results for the case of 0^0 to 25^0 incident angle disclosed that the magnitude of the reflectivity for both the TE and TM cases is below the -10dB reference level for the whole bandwidth recorded under normal incidence as could be seen in Fig. 4a and 5a respectively. Specifically, for TE polarization, it is obvious from Fig. 4a that the reflection frequency is blue shifted as the absorption peaks increases. Also, the absorption peaks decrease with the increase of angle of incidence. Therefore, our simulation results proves the frequency and incident angle dependence of the absorption characteristics of metamaterial absorbers when we consider Equation (6) proposed by (Yang et al., 2017). The proposed equation was validated using dielectric substrate based metamaterial absorber (Yang et al., 2017) and revalidated by our magnetic substrate based RAM with metamaterial features which signifies its effectiveness in describing MMAs. Meanwhile, the structure performance was theoretically evaluated in order to further confirm its reliability and consequential validation of its performance under oblique incidence. The results seem to be consistent as revealed in Fig. 4a and 4b despite the slight deviations in reflectivity peaks. This could be ascribed to the amount of incident wave received by the surface layers of the simulated and theoretical models. The surface layer of the theoretical model is expected to receive all the incident wave striking the absorber, while a fraction of the incident wave finds its way to the underneath layers in the simulated model due to its cross-shaped structure.

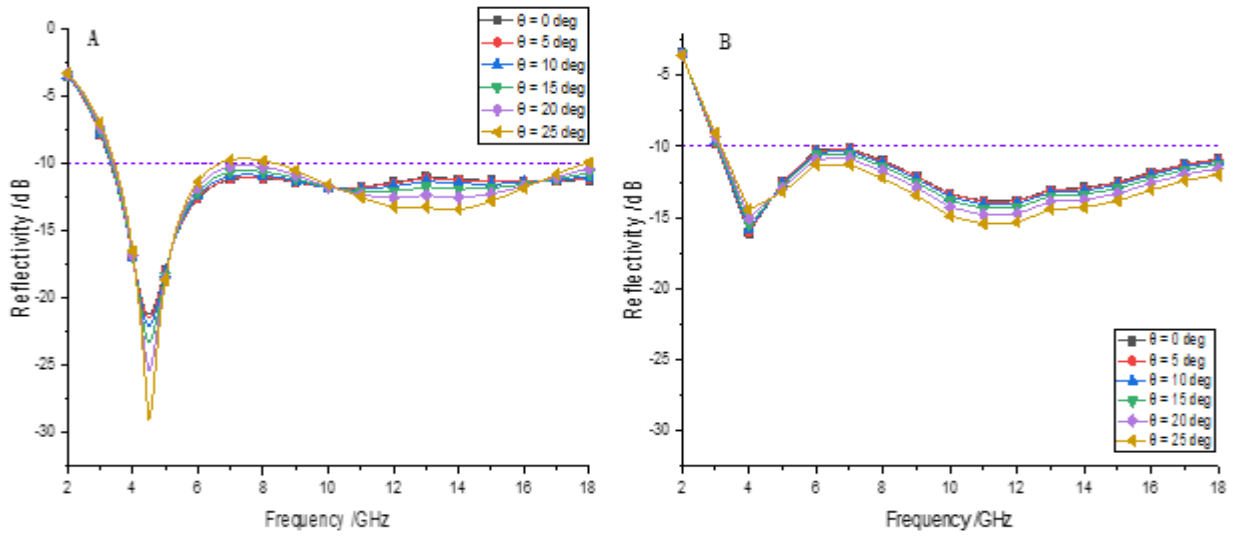

Fig. 5: Reflectivity plots for TM polarization at oblique incidence (a) simulated (b) calculated

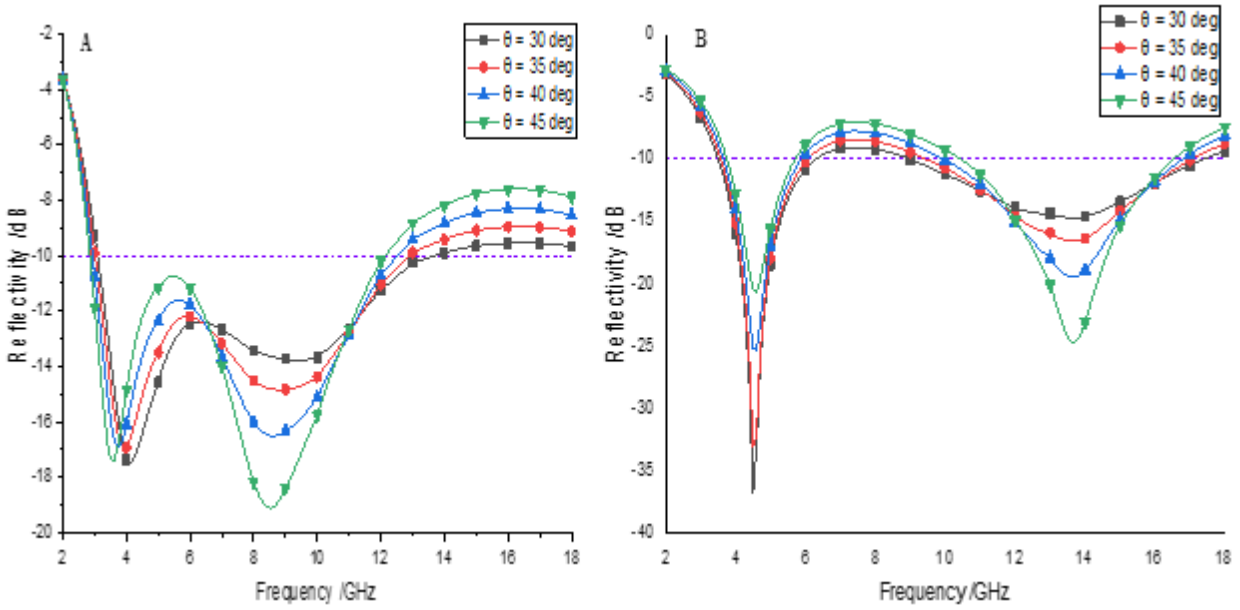

Fig. 6: Simulated reflectivity plots at oblique incidence for (a) TE and (b) TM polarizations

For the TM polarization, the simulated and calculated reflectivity intensities increase with the increase of angle. Just like in the case of TE polarization, the simulated (Fig. 5a) and calculated (Fig. 5b) reflectivity curves are in agreement for the angles of incidence considered. Nevertheless; for angles of incidence ranging from 30^0 to 45^0, slight changes in the magnitude of the reflectivity for the TE and TM polarization were observed. Wherein reflectivity reaches a lowest value of -7.5dB (82% absorption) for the TE polarization as shown in Fig. 6a, it attains a least value of -7dB (80% absorption) for the TM polarization as revealed in Fig. 6b. It is also observed that the bandwidth of below -10dB is 9.4 GHz and 8.3 GHz obtained in a single and dual band for TE and TM polarizations respectively. It is noteworthy that despite this minor setback, the absorptivity remains higher than 80% for all cases, which means that stability is achieved and the structure can be described as a wide angle of incidence absorber.

To show that the structured radar absorbing material exhibit metamaterial features, a conventional absorber of same material and thickness was simulated to obtained its absorption characteristics. It is obvious from the results in Fig. 7 that the designed radar absorber is effectively homogenous, behaves unconventionally and its absorption behaviour is dependent on its geometric dimensions which qualifies it to be a metamaterial based on the general definition of metamaterials (Caloz and Itoh, 2006). The radar absorber's unit cell size of 0.17λ satisfies the effective homogeneity condition of $\leq 0.25\ \lambda$ (Caloz and Itoh, 2006), thereby exhibiting metamaterial feature. The reflectivity property of the designed RAM clearly surpassed the unstructured single layer conventional one, designed from same material and thickness. It is clear from Fig. 7 that the reflectivity is below -10dB benchmark in the 2-3 GHz only for the conventional, but the present structured radar absorber demonstrates the below -10dB reflectivity in the entire 3-18 GHz for both normal and oblique incidence. Thus, the structured radar absorber behaves unconventionally when compared to its counterpart conventional absorber; hence, it showcases metamaterial feature. Likewise, another metamaterial feature demonstrated by our radar absorber is its reflection property dependence on its geometrical dimension leading to an optimized dimension of the structure used in the design.

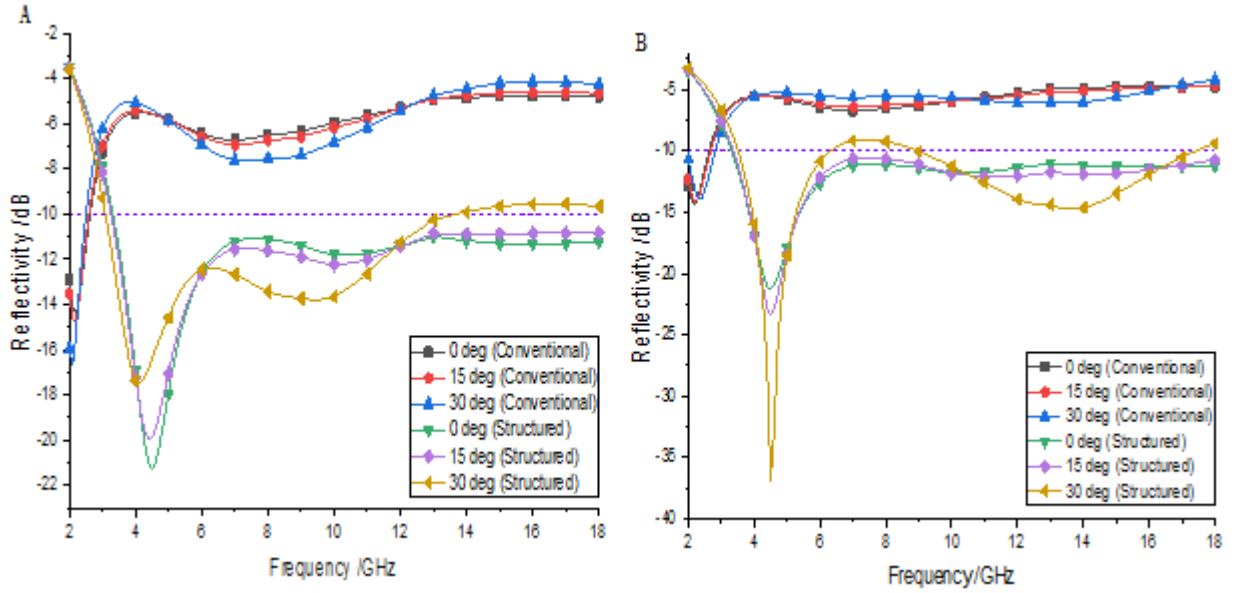

Fig. 7: Simulated reflectivity plots of structured and conventional absorbers for (a) TE and (b) TM polarization at normal and oblique incidence

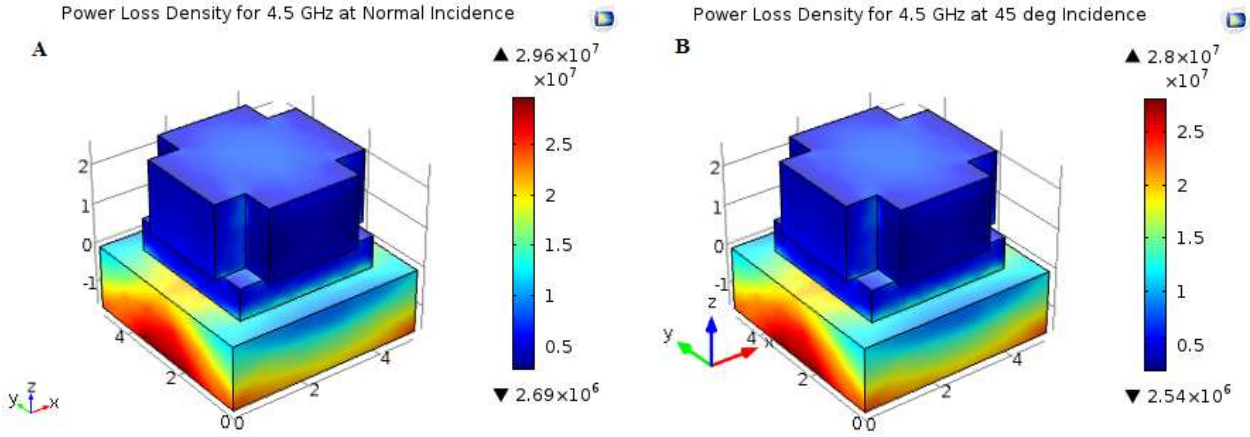

Fig. 8: Power loss density distribution at 4.5 GHz for TE polarization under (a) normal incidence (b) 45^0 incidence.

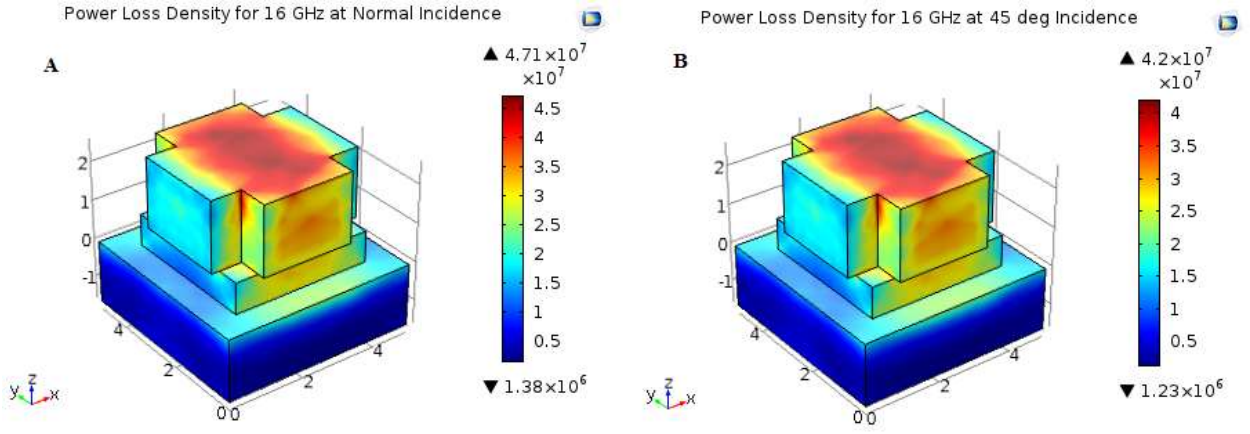

Fig. 9: Power loss density distribution at 16 GHz for TE polarization under (a) normal incidence (b) 45^0 incidence.

Table 1: Performance comparison with metamaterial absorbers at normal and oblique incidence

		Normal Incidence			**Oblique Incidence (45^0)**		
References	Thickness (mm)	Relative Thickness	Relative Bandwidth	Effective Bandwidth (GHz)	Relative Thickness	Relative Bandwidth	Effective Bandwidth (GHz)
Haitao et al., 2018	2.0	0.045	2.38	9.79	Nil	Nil	Nil
Cheng et al., 2016	2.0	0.017	2.08	2.70	Nil	Nil	Nil
Wangchang et al., 2018	2.0	0.027	1.40	1.60	Nil	Nil	Nil
Chen et al., 2016	2.2	0.018	2.24	3.10	0.025	1.12	0.80
This Work	4.2	0.048	5.29	14.6	0.039	4.35	9.40

To investigate the physical mechanism of the absorption property of the present RAM, we studied the power loss density distributions at the frequencies of 4.5 GHz and 16 GHz representing the absorption peaks at lower and higher frequencies of the absorber's operating frequency band. Fig. 8a and 8b depicts power loss density distributions for TE polarization at 4.5 GHz under normal and oblique incidence respectively, while Fig. 9a and 9b indicates that of 16 GHz under normal and oblique incidence respectively for TE polarization. It can be observed clearly that the strong power loss at the lower frequency (4.5 GHz) is mainly focused around the central position of the bottom layer which corresponds to the cross-shaped surface layer position along x-axis. A maximum power loss value of 2.96×10^7 W/m^3 is achieved as revealed in Fig. 8a which is the case of normal incidence. Similarly, the strong power loss at the higher frequency (16 GHz) is mainly focused on the cross-shaped surface layer and the power loss peak value is 4.71×10^7 W/m^3, as shown in Fig. 9a. This clearly indicates that the structure improves the absorption characteristics of CIF magnetic composite which is known to be weak at lower frequencies (2-8 GHz) (Li et al., 2014) by offering appropriate impedance matching condition via the shape and geometrical dimension of the structure. The incident lower frequencies are guided to the bottom layer where they are efficiently absorbed while the higher frequencies are efficiently absorbed at the surface layer. When the structure receives TE polarized radar frequencies at 45^0 to the normal, the power loss density pattern is maintained though with slightly diminished values of 2.8×10^7 W/m^3 and 4.2×10^7 W/m^3 at 4.5 GHz and 16 GHz respectively according to Fig. 8b and 9b results.

The performance of the proposed MMA is compared with that of other MMAs that are numerically and experimentally realized (Chen et al., 2016; Cheng et al., 2016; Haitao et al., 2018; Li et al., 2018) as shown in Table 1. Compared with other MMAs in the literature listed in table 1, the RAM with metamaterial features reported in this paper has good relative thickness, better relative bandwidth level and wider effective bandwidth for both the normal and oblique incidence conditions. Relative bandwidth is the ratio of the highest frequency to the lowest frequency in absorption band while relative thickness is the ratio of the thickness to wavelength of the lowest frequency in absorption band. Moreover, the proposed RAM has the advantages of small thickness compared to broadband absorbers (Yi-jun et al., 2018; Zhang et al., 2014; Zhou et al., 2016), broadband absorption characteristics and wide angle of incidence property.

5. Conclusions

The proposed structure improves the absorption characteristics of the magnetic composite employed in the design. Simulation results of reflection spectra under different incident angles revealed that the RAM structure works well for TE and TM waves for the incident angles in the range of 0^0–45^0. The absorption band for reflectivity below −10 dB of the structure with a 4.2 mm total thickness covers the frequencies range of 3.4 GHz to 18.0 GHz under normal incidence, but decrease to within the range of 2.8 GHz to 12.2 GHz at 45^0 angle of incidence. However, the absorptivity remains higher than 80% for all cases, which means that stability is realized under oblique

incidence and the structure can be described as a wide angle of incidence metamaterial absorber. Moreover, the proposed RAMM has relatively wider relative bandwidth compared to the currently published structures reviewed, with a competitive relative bandwidth of 5.2 (at normal incidence) and 4.35 (at 45^0 incidence) for TE polarization. Finally, the developed RAMM has potentials to be used in practice in multiple electromagnetic applications like stealth technology and wireless communication.

References

Abdalla, M.A. (2013) Experimental verification of a triple band thin radar absorber metamaterial for oblique incidence applications. Progress in Electromagnetics Research Letters, 39(4): 63–72.

Abdullahi, M.B. and Ali, M.H. (2019) Design and Simulation of Cross-Block Structured Radar Absorbing Metamaterial Based on Carbonyl Iron Powder Composite. Nigerian Journal Of Technology, 38(4): 912–918.

Caloz, C. and Itoh, T. (2006) Electromagnetic metamaterials: transmission line theory and microwave applications: the engineering approach. In Wiley-Interscience, John Wiley & Sons Inc.

Chen, Q., Bie, S., Yuan, W., Xu, Y., Xu, H. and Jiang, J. (2016) Low frequency absorption properties of a thin metamaterial absorber with cross-array on the surface of a magnetic substrate. Journal of Physics D: Applied Physics, 49: 425102.

Cheng, Y., He, B., Zhao, J. and Gong, R. (2016) Ultra-thin Low-Frequency Broadband Microwave Absorber Based on Magnetic Medium and Metamaterial. Journal of Electronic Materials, 46(2): 1293-1299.

Cheng, Y., Nie, Y., Wang, X., Gong, R., Cheng, Y., Nie, Y., Wang, X. and Gong, R. (2014) Adjustable low frequency and broadband metamaterial absorber based on magnetic rubber plate and cross resonator Adjustable low frequency and broadband metamaterial absorber based on magnetic rubber plate and cross resonator. Journal of Applied Physics, 115(6), 064902–1 to 064902–064905.

Dib, N., Asi, M. and Sabbah, A. (2010) On the optimal design of multilayer microwave absorbers. Progress In Electromagnetics Research, 13: 171–185.

Edwards, B., Alù, A., Silveirinha, M. G. and Engheta, N. (2009) Experimental verification of plasmonic cloaking at microwave frequencies with metamaterials. Physical Review Letters, 103(15): 153901-1 to 153901-4.

Haitao, G., Jiangjiang, W., Baocai, X., Ze, L. and Qingtao, S. (2018) Broadband metamaterial absorber based on magnetic substrate and resistance rings. Materials Research Express, 6(4): 045803.

Hokmabadi, M.P., Wilbert, D.S., Kung, P. and Kim, S.M. (2013) Design and analysis of perfect terahertz metamaterial absorber by a novel dynamic circuit model. Optics Express, 21(14): 16455–16465.

Kapelewski, J. (2013) On current and prospective use of binary thin multilayers in radar absorbing structures. Acta Physica Polonica, 124(3): 451-455.

Landy, N.I., Sajuyigbe, S., Mock, J.J., Smith, D.R. and Padilla, W.J. (2008) Perfect metamaterial absorber. Physical Review Letters, 100(20): 1–4.

Li, W., Liu, Q., Wang, L., Zhou, Z., Zheng, J., Ying, Y., Qiao, L., Yu, J., Che, S., Li, W., Liu, Q., Wang, L., Zhou, Z. and Zheng, J. (2018) Low frequency and broadband metamaterial absorber with cross arrays and a flaked iron powder magnetic composite Low frequency and broadband metamaterial absorber with cross arrays and a flaked iron powder magnetic composite. AIP Advances, 8(1): 015318–1 to 015318–015319.

Li, W., Wu, T., Wang, W., Guan, J. and Zhai, P. (2014) Integrating non-planar metamaterials with magnetic absorbing materials to yield ultra-broadband microwave hybrid absorbers. Applied Physics Letters, 104(2): 16–21.

Liu, X., Tyler, T., Starr, T., Starr, A. F., Jokerst, N. M., & Padilla, W. J. (2011). Taming the Blackbody with Infrared Metamaterials as Selective Thermal Emitters. Physical Review Letters, 107(4), 045901.

Luo, H., Chen, F., Wang, X., Dai, W., Xiong, Y., Yang, J. and Gong, R. (2019) A novel two-layer honeycomb sandwich structure absorber with high- performance microwave absorption. Composites Part A, 119: 1–7.

Mulla, B. and Sabah, C. (2015) Perfect metamaterial absorber design for solar cell applications. Waves in Random and Complex Media, 25(3): 382–392.

Nguyen, T.T. and Lim, S. (2018) Angle- and polarization-insensitive broadband metamaterial

absorber using resistive fan-shaped resonators. Applied Physics Letters, 112(2): 021605.

Pang, Y., Cheng, H., Zhou, Y., Li, Z. and Wang, J. (2012) Ultrathin and broadband high impedance surface absorbers based on metamaterial substrates, 20(11): 12515–12520.

Ranjan, P., Choubey, A. and Mahto, S.K. (2018) A novel approach for optimal design of multilayer wideband microwave absorber using wind driven optimization technique. AEU - International Journal of Electronics and Communications, 83: 81–87.

Smith, D.R., Padilla, W.J., Vier, D.C., Nemat-Nasser, S.C. and Schultz, S. (2000) Composite medium with simultaneously negative permeability and permittivity. Physical Review Letters, 84(18): 4184–4187.

Tao, H., Bingham, C.M., Strikwerda, A.C., Pilon, D., Shrekenhamer, D., Landy, N.I., Fan, K., Zhang, X., Padilla, W.J. and Averitt, R.D. (2008a) Highly flexible wide angle of incidence terahertz metamaterial absorber : Design , fabrication , and characterization. Physical Review B, 78(4): 2–5.

Tao, H., Strikwerda, A.C., Fan, K., Bingham, C.M., Padilla, W.J., Zhang, X. and Averitt, R.D. (2008b) Terahertz metamaterials on free-standing highly-flexible polyimide substrates. J. Phys. D: Appl. Phys., 41: 1–5.

Wan, D., Bie, S., Zhou, J., Xu, H., Xu, Y. and Jiang, J. (2015) A Thin and Broadband Microwave Absorber Based on Magnetic Sheets and Resistive FSS. Progress In Electromagnetics Research C, 56(2): 93–100.

Wiltshire, M.C.K., Pendry, J.B., Young, I.R., Larkman, D.J., Gilderdale, D.J. and Hajnal, J.V. (2001) Microstructured magnetic materials for rf flux guides in magnetic resonance imaging. Science, 291(5505): 849–851.

Wong, S.K., Riseborough, E., Duff, G. and Chan, K.K. (2006) Radar cross-section measurements of a full-scale aircraft duct/engine structure. IEEE Transactions On Antennas And Propagation, 54(8): 2436–2441.

Xiao, H., Qu, Z., Lv, M., Du, H., Zhu, W., Wang, C. and Qin, R. (2019) Optically transparent broadband and polarization insensitive microwave metamaterial absorber. Journal of Applied Physics, 126(13): 135107-1 to 135107-8.

Xu, H., Bie, S., Xu, Y., Yuan, W., Chen, Q. and Jiang, J. (2015) Broad bandwidth of thin composite radar absorbing structures embedded with frequency selective surfaces. Composites Part A.

Xu, Y., Yuan, W., Bie, S., Xu, H., Chen, Q. and Jiang, J. (2015) Broadband microwave absorption property of a thin metamaterial containing patterned magnetic sheet. Journal of Electromagnetic Waves and Applications, 29(18): 2420–2427.

Yang, C., Xiong, H. and Li, X.P. (2017) Investigation of a metamaterial absorber by using reflection theory model, 59(August): 65–73.

Yi-jun, X., Wang, Y., Wang, Q., Chun-Qi, W., Xiao-Zhong, H., Fen, Z. and Ding, Z. (2018) Structural broadband absorbing metamaterial based on three-dimensional printing technology. Acta Physica Sinica, 67(8): 084202-1 to 084202-8.

Zhang, L., Zhou, P., Chen, H., Lu, H., Xie, J. and Deng, L. (2015) Ultra-thin wideband magnetic-type metamaterial absorber based on LC resonator at low frequencies. Applied Physics A: Materials Science and Processing, 121(1): 233–238.

Zhang, L., Zhou, P., Zhang, H., Lu, L., Zhang, G., Chen, H., Lu, H., Xie, J. and Deng, L. (2014) A Broadband Radar Absorber Based on Perforated Magnetic Polymer Composites Embedded With FSS. IEEE Transactions on Magnetics, 50(5): 1-5.

Zhou, D., Huang, X. and Du, Z. (2017) Analysis and design of multi-layered broadband radar absorbing metamaterial using 3D printing technology-based method. IEEE Antennas and Wireless Propagation, 16: 1–4.

Zhou, D., Huang, X., Du, Z. and Wang, Q. (2016) Calculation and analysis of the effective electromagnetic parameters of periodic structural radar absorbing material using simulation and inversion methods, 52(October): 57–66.